EASR

Engineering and Applied Science Research

https://www.tci-thaijo.org/index.php/easr/index

Published by the Faculty of Engineering, Khon Kaen University, Thailand

Design and development of multi-band multi-generation compatible MIMO antenna for wireless devices

Arumita Biswas*[1,2] and Vibha Rani Gupta[1]

[1]Department of Electronics and Communication Engineering, Birla Institute of Technology, Mesra, Ranchi,835215 India
[2]Cellular Mobile Telephone Services Department, Bharat Sanchar Nigam Limited, Kolkata, 700013, India

Received 13 June 2019
Revised 21 September 2019
Accepted 30 September 2019

Abstract

A planar dual-element multi-generation compatible MIMO antenna is presented in this paper. The radiating antenna elements are designed to resonate over two frequency ranges: 1.41 GHz – 2.11 GHz and 3.6 GHz – 3.8 GHz, with (S_{11}/S_{22}) reference considered as -10 dB,covering frequencies allotted for L1 GPS, 2G standards (GSM-1800 and GSM-1900), 3G standard (UMTS), LTE (working on TDD and FDD techniques) and 5G New Radio. The designed antenna is optimized using IE3D simulation software and fabricated on FR4 substrate having relative permittivity of 4.4, loss tangent of 0.02 and thickness of 1.6 mm. A three step isolation improvement and impedance bandwidth enhancement technique is presented to reduce the mutual coupling and cover the desired frequency range. Antenna characteristics in terms of the reflection coefficient, mutual coupling, radiation pattern and gain are measured and show good agreement with the simulated results. Diversity performance is evaluated in terms of the envelop correlation coefficient. It is found to be less than 0.12 and 0.06 in the first and second bands of frequencies, respectively. The planar structure and capability to support several frequencies of multiple generations make the proposed MIMO antenna a good candidate for integration with future wireless devices.

Keywords: Envelop correlation, Isolation improvement, Multiband antenna, Multi-generation antenna, Monopole antenna, MIMO antenna

1. Introduction

Mobile communication has revolutionized the communication industry. Ever since its first introduction as1st generation analogue mobile communication standard, several technologies have been introduced to lead to generations such as 2G, 2.5G, 2.75G , 3G, 3.5G, 3.65G and likewise to the current Long Term Evolution (LTE). With each of these successive generations, the spectrum allocation, key technologies, system requirement and services provided to the subscribed users varied. The 1st generation standards like Advanced Mobile Phone Service (AMPS) and Total Access Communication System (TACS) offered only voice call services. The 2nd generation standards were based on digital techniques and offered voice and text messaging services. From 2.5 generation standards to the current 4G standards, the main aim was to provide higher rate data service, increased capacity and reduced latency [1-2]. Currently, subscribers enjoy real-time voice, data, multimedia and short messaging services [3]. Most telecom operators allow their subscribed users to switch between 2G,3G and LTE services as per user's demand and network strength. While registered subscibers latch to a 2G network during accessing voice service, they prefer to latch to 3G network and beyond for accessing high speed data service [2,4]. However even deployment of a 4G communication system could not meet the increasing demand of data speed. Researchers all over the globe are currently working towards the development and standardization of 5G communication technology [5-6]. 3GPP in release 15 has proposed two wide ranges of frequency spectrum that can be employed for 5G services –FR1 and FR2. The FR1 band, also referred to as sub-6 GHz band, ranges between 450 MHz and 6 GHz, while the FR2 band, also referred to as the mm-Wave band, ranges between 24.25 GHz and 52.6 GHz. FR1 is comprised of a total of 27 bands, of which 12 bands are based on Frequency Division Duplexing (FDD), 7 bands are based on Time Division Duplexing (TDD), 6 bands are based on Suplementary UpLink (SUL) and 2 bands are based on Suplementary DownLink (SDL) techniques. [7- 8]. The World RadioCommunication Conference (WRC) is organised by ITU every three to four years to review the allocation of frequency spectrum for various services. Allocation of t 3.5 GHz C-band at WRC 2015 for 5G antenna structure and beamforming further triggerred research all over the globe. With these speedy developments, wireless communication networks have formed into a heterogeneous networks working on various standards of different generations that are allotted a varied portion of the frequency spectrum [9]. As a result, designing a wireless

*Corresponding author.
Email address: arumita.jto@gmail.com
doi: 10.14456/easr.2020.7

Table 1 Mobile communication standards supported by the proposed dual-element MIMO antenna

S. No.	Mobile Communication Standards/ Generations	Bands
1	GPS	L1-GPS
2	2G	GSM 1800, GSM 1900
3	3G	UMTS
4	LTE FDD	B2, B3, B9, B11,B21,B24, B25, B32
5	LTE TDD	B33, B34, B35, B36, B37, B39, B43
6	Partial LTE bands	B1, B4, B10
7	5G New Radio	n2, n3, n25, n34, n39, n51, n70, n74, n75, n76, n80, n84, n86
8	Partial 5G New Radio	n1, n66, n77, n78

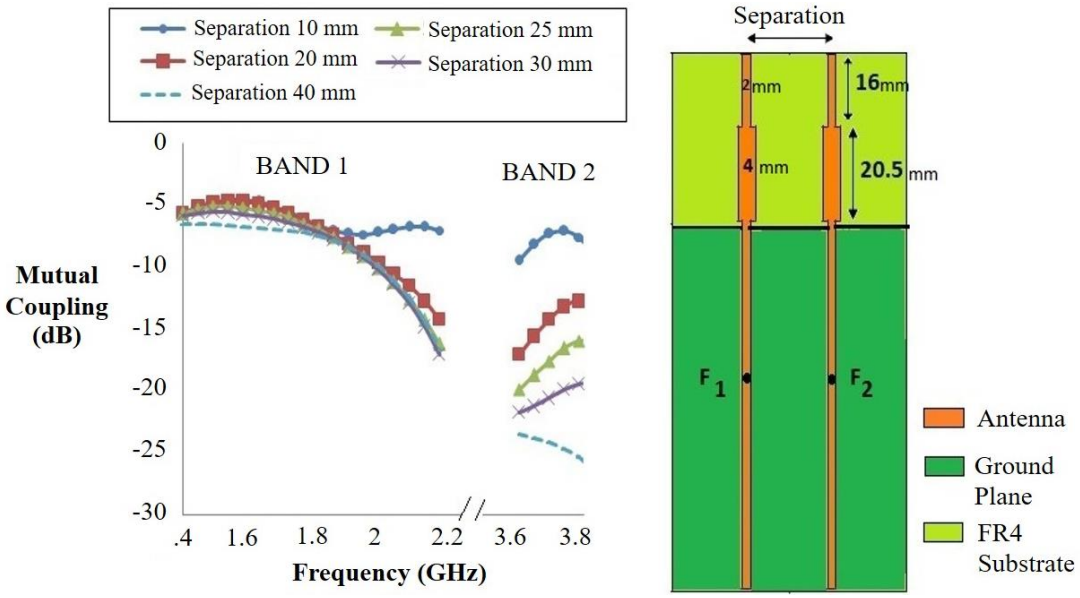

Figure 1 Effect on mutual coupling with increased separation between identical antenna elements

device that can support multiple generations is a pressing current need.

Antenna systems have undergone major enhancements to fit to the requirements of various mobile communication standards. A multiband antenna should be designed to support different generations of mobile communication working on various frequencies [3]. In order to enhance the data speed, a shift from Single Input Single Output (SISO) to Multiple Input Multiple Output (MIMO) antenna system is greatly needed. Theoretically, the capacity of an MIMO antenna system employing more than one antenna at transmitting and receiving end, should linearly increase with increase in the number of elements in the antenna system.However,in reality,correlation between the antenna elements affects the enhancement in system capacity [10-12]. Hence, in any MIMO antenna design, reduction of mutual coupling between the elements is an important criterion. In the sub-6 GHz spectrum range, a 10 dB isolation level is considered acceptable for a 5G MIMO.However,to achieve better performance, a higher isolation level is desired [13]. Various techniques have been investigated by researchers to improve the isolation between identical antennae in multi-element antenna configurations,such as introduction of a neutralization line [14-15], introducing a ground extension to extend the length of surface current [16], designing parasitic elements [17] and using pattern diversity [18]. Several researchers have proposed different antennae that find use in mobile communications. Both SISO [19-25] and MIMO antenna configurations [3-6, 9, 12-14, 18, 26-31] have been proposed by researchers.While some researchers have adopted the benchmark of S_{11}/S_{22} less than -6 dB [4, 6, 14, 19-21, 23-25, 29, 31], others have not designed antennas to include frequencies of all generations of mobile communication [3-6, 9, 12-14, 18-22, 24-33].

In this paper, a simple planar dual-element MIMO antenna is proposed that can be used over L1 GPS, 2G standards such as GSM-1800 and GSM-1900, 3G standard UMTS working on 2.1 GHz, several LTE bands working on both TDD and FDD techniques and several 5G New Radio frequencies. Table 1 lists the standards of the corresponding mobile generations over which the proposed antenna can be employed. The radiating elements cover these bands with S_{11} and S_{22} less than -10 dB reference. In the following section, antennae are designed to develop the unit antenna element. Isolation and impedance bandwidth improvement techniques incoporated in a dual-element MIMO system to achieve isolation better than 10 dB for all frequencies under consideration is included.Simulated and measured results in terms of the reflection coefficient, mutual coupling, gain and radiation pattern have been investigated. Diversity performance in terms of the Envelop Correlation Coefficient (ECC) has been examined and a comparison with existing work has been done. Finally, the conclusionsof the obtained results are presented.

2. Antenna configuration

The length of monopole antenna resonating at 'f' Hz and wavength 'λ' is computed using equation (1) below:

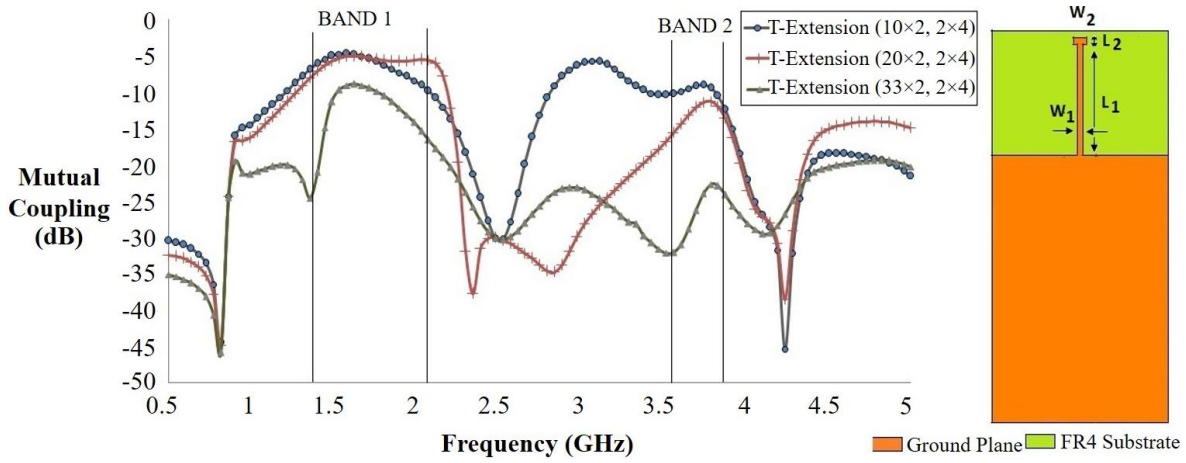

Figure 2 Effect on mutual coupling by varying the length of a T-shaped ground extension

$$L = \lambda/4 = c/4f \quad (1)$$

where,
c = velocity of light = 3 x 10^8 m/sec

For designing unit antenna elements to work on frequencies covered by L1 GPS, 2G, 3G, LTE and 5G New Radio, two ranges of frequencies were considered; the first band from 1.4 GHz to 2.7 GHz, while the second from 3.4 GHz to 3.8 GHz. The center frequencies for both the bands were computed as 2.05 GHz and 3.6 GHz, respectively. Using (1), the resonant length of each monopole antenna elements corresponding to the centre frequencies were obtained as 36.5 mm and 20.8 mm, respectively. These different computed lengths of monopole antennae with varying widths were superimposed to design a single multiband antenna structure. The final unit antenna element was a single non-uniform width monopole element. A parametric study was conducted to select the ground plane dimension. In the final geometry, after optimization, a ground plane of dimension 55 mm x 80 mm was considered. For designing the MIMO antenna system, two such identical unit antenna elements were placed beside each other and the input was fed using 50 ohm coaxial probe. It was observed that in the designed dual-element MIMO antenna, the two superimposed lengths of monopole antenna radiated over two bands ranging from 1.47 – 2.12 GHz and 3.7 – 3.87 GHz considering S_{11} and S_{22} < -10 dB. However, due to the close proximity of the unit antennas, there was huge mutual coupling (- 4.55 dB in first band and -7.05 dB in second band). This in turn rendered the MIMO antenna system inefficient. A three step enhancement method was employed to enhance the isolation between the antenna elements and improve the impedance bandwidth.

First, the separation between the elements was increased. In an MIMO antenna setup, the multi-paths between the transmitter and receiving antenna require to be highly un-correlated to enhance performance. One of the easiest ways to achieve de-correlation is to increase the separation between the antennae. The separation was gradually increased from 10 mm to 40 mm and its effect on antenna performance was recorded. Figure 1 illustrates the basic dual-element MIMO antenna setup and the mutual coupling obtained on increasing the antenna element separation. From the figure, it can be seen that for the second band for separation above 15 mm, mutual coupling was less than -10 dB. However, for the first band, the mutual coupling value was much above desired threshold. Moreover, due to size constraints, further separation of antenna elements was not possible.

A T-shaped ground extension was next introduced between the unit antenna elements in the MIMO setup to reduce mutual coupling in both the bands. Figure 2 illustrates comparative plots of the mutual coupling obtained in three scenarios when T-shaped extensions of different lengths were introduced. These are test case 1 with L_1, W_1, L_2, W_2 as 10 mm, 2 mm, 2 mm, and 4 mm. Test case 2 with L_1, W_1, L_2, W_2 as 20 mm, 2 mm, 2 mm, and 4 mm. Test case 3 with L_1, W_1, L_2, W_2 as 33 mm, 2 mm, 2 mm, and 4 mm, respectively. The introduction of a ground extension aided in increasing the length of the surface current, which in turn reduced the mutual coupling between the identical elements in both bands, keeping the separation fixed at 20 mm. In the third test case, in both the desired bands, mutual coupling lower than -10 dB was obtained. However, the impedance bandwidth still required improvement to cover the frequencies of mobile communication standards under consideration without degrading the isolation between elements. So, decoupling line and ground slot were introduced to improve the impedance bandwidth. The dimension of the slot and the length of the decoupling line were optimized in IE3D software. Figure 3 illustrates the effect of introduction of the optimized decoupling line and ground slot. Hence, by using the three step isolation and impedance bandwidth improvement technique, it was possible to design a final dual-element MIMO antenna system. The final version of the dual element MIMO antenna radiated over two bands of frequencies ranging between 1.41 GHz – 2.11 GHz and 3.6 GHz – 3.8 GHz, with a (S_{11}/S_{22}) reference of -10 dB and mutual coupling lower than the threshold of -10 dB over the entire range. As a validation of this statement, Figure 4 illustrates the comparative mutual coupling plots. They were first recorded with no isolation technique and then they were obtained with the proposed hybrid technique.

The simulated current distribution was investigated in two scenarios to study the performance of the designed MIMO structure. The first was without any isolation improvement, while the second employed the hybrid technique. Owning to the symmetry of the designed dual-element MIMO antenna for an investigation input port (F_2) of Ant 2was excited while the input port (F_1) of Ant 1 was terminated with a matched load. Figure 5 illustrates the simulated current distribution output recorded for the two sample frequencies, 1.8 GHz and 3.7 GHz, one frequency being considered from both the bands over which

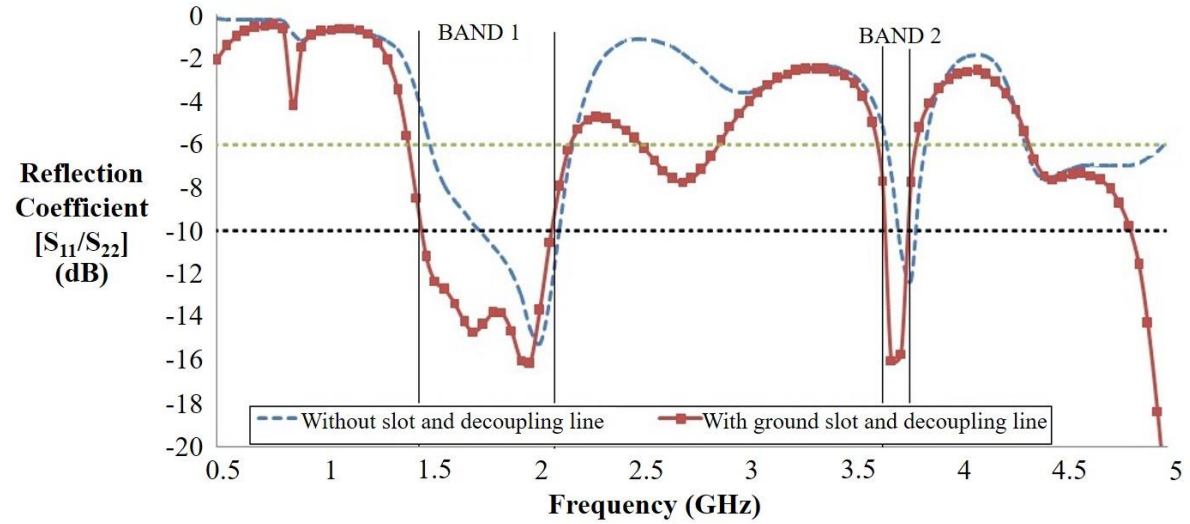

Figure 3 Effect of introduction of a ground slot and decoupling line

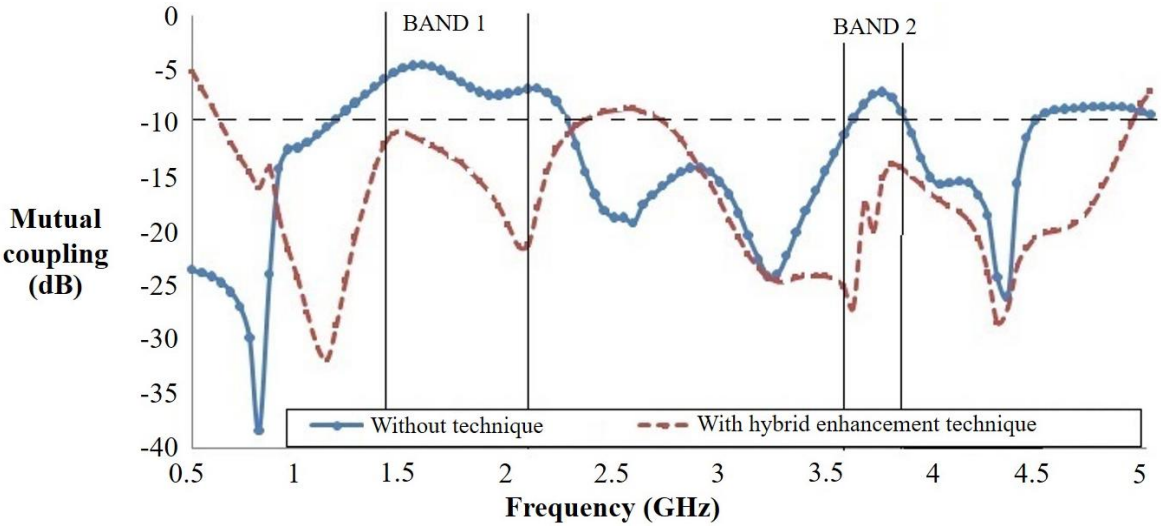

Figure 4 Mutual coupling comparative plots with and without hybrid isolation and impedance bandwidth enhancement technique

the antenna element resonates. It can be observed that for the first frequency, 1.8 GHz, the current distribution is dominant in the upper section of the monopole, while for the second frequency, 3.7 GHz, the current distribution is dominant in the lower section of the monopole. Furthermore, it can be observed that in both the cases, there is negligible current concentration on Ant 1 when port 2 is excited and the hybrid technique designed has been introduced between the dual-element MIMO representing good isolation improvement.

The front and back planes of the final designed MIMO antenna prototype are illustrated in Figure 6a, with all dimensions mentioned being in 'mm'. The optimized ground plane dimension is (L_G x W_G) 80 mm x 55 mm, while the non-ground area is 37 mm x 55 mm. F_1 and F_2 in the figure indicate the two feeding points, where the 50 ohm input probes are connected. The designed antenna was simulated and optimized using IE3D software. A double side copper-clad FR4 substrate with a dielectric constant (ε_r) of 4.4, thickness (h) of 1.6 mm and loss tangent (tan δ) 0.02 was used for fabrication. Figure 6b illustrates the front and back planes of the final fabricated antenna prototype.

3. Results and discussion

In this section, the antenna's performance in terms of its reflection coefficient, mutual coupling, radiation characteristics and gain are discussed. Diversity performance of the designed MIMO antenna is discussed in terms of ECC. The section further highlights the significance of the designed antenna over previous efforts.

3.1 Reflection coefficient and mutual coupling

For measuring the impedance performance in terms of the reflection coeffcient and mutual coupling, the fabricated antenna was connected to a Network Analyzer, Agilent Technologies N5230A 10MHz-20GHz PNA-L. Figure 7a illustrates the setup used for measuring S_{11}, S_{22}, S_{12}, S_{21} parameters. Figure 7b illustrates a comparison between the simulated and measured reflection coefficient (S_{11}, S_{22}) characterictics. Taking the S_{xx} level as less than -10 dB, this proposed antenna resonates over two frequency ranges,1.41 GHz to 2.11 GHz with minimum of -27.3 dB at 1.6 GHz and 3.6 GHz to 3.8 GHz with minimum of -41.7 dB

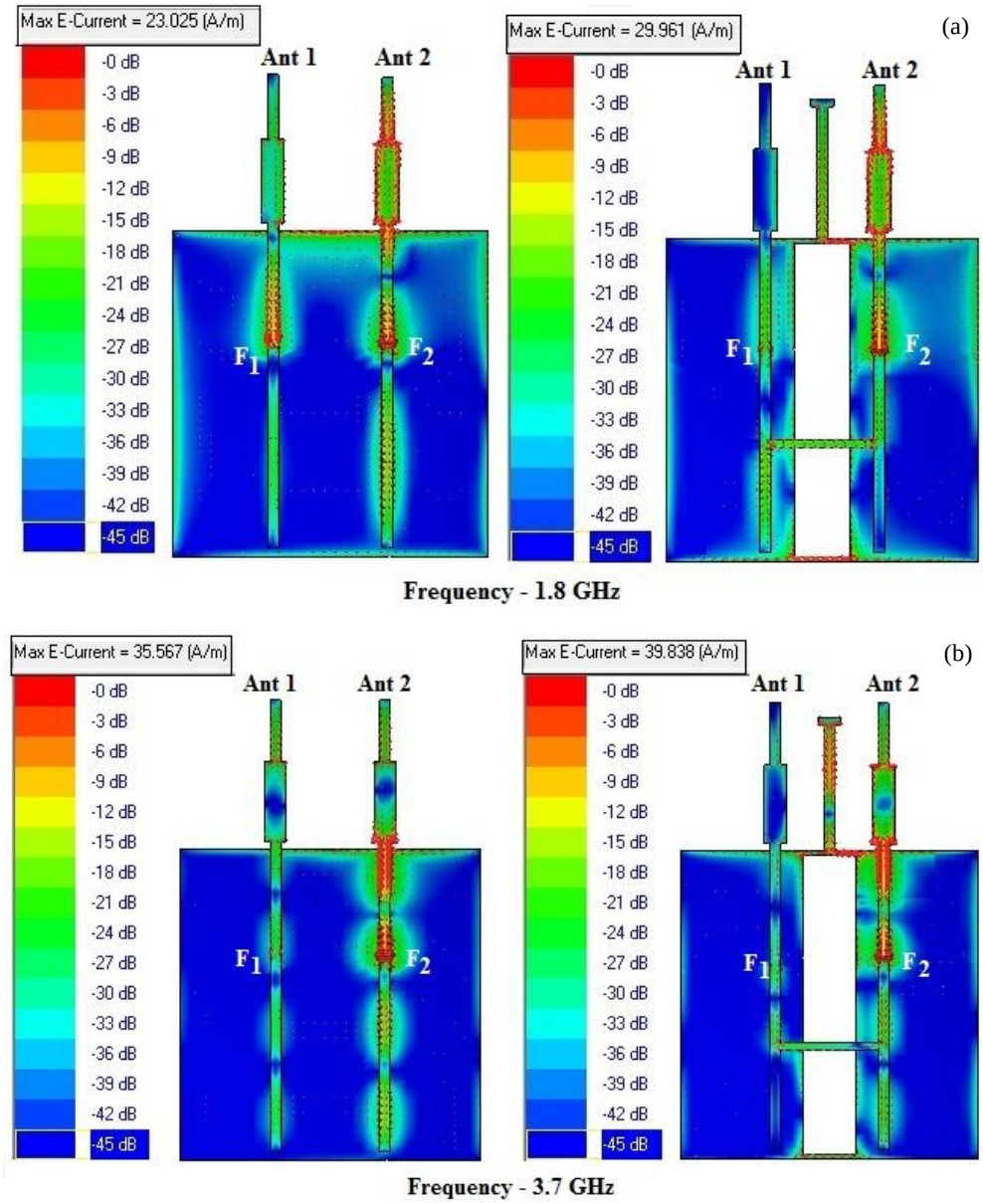

Figure 5 Simulated current distributions recorded with and without proposed hybrid isolation and impedance enhancement technique with port F_2 excited and port F_1 terminated with a matched load at (a) 1.8 GHz and (b) 3.7 GHz

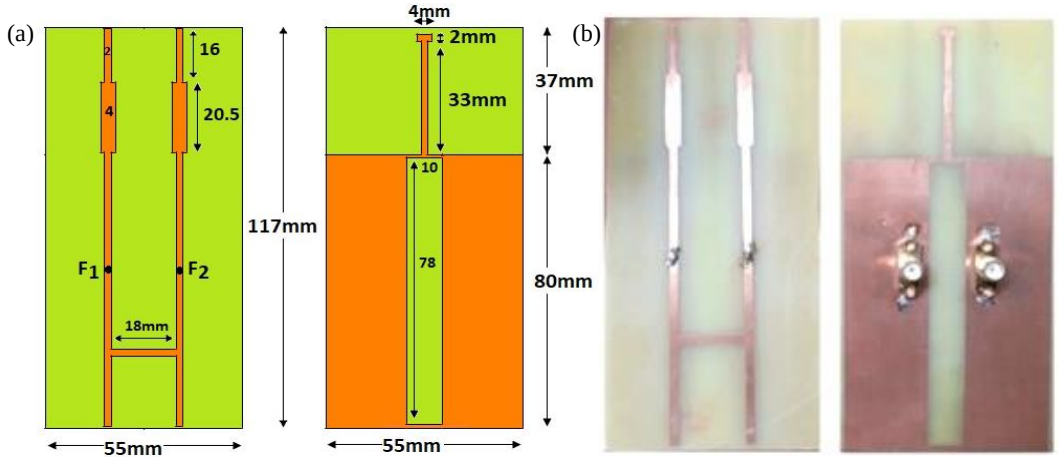

Figure 6 Final MIMO antenna prototype: (a) Front and back plane geometry with dimensions in mm, (b) Fabricated front and back plane on a FR4 substrate

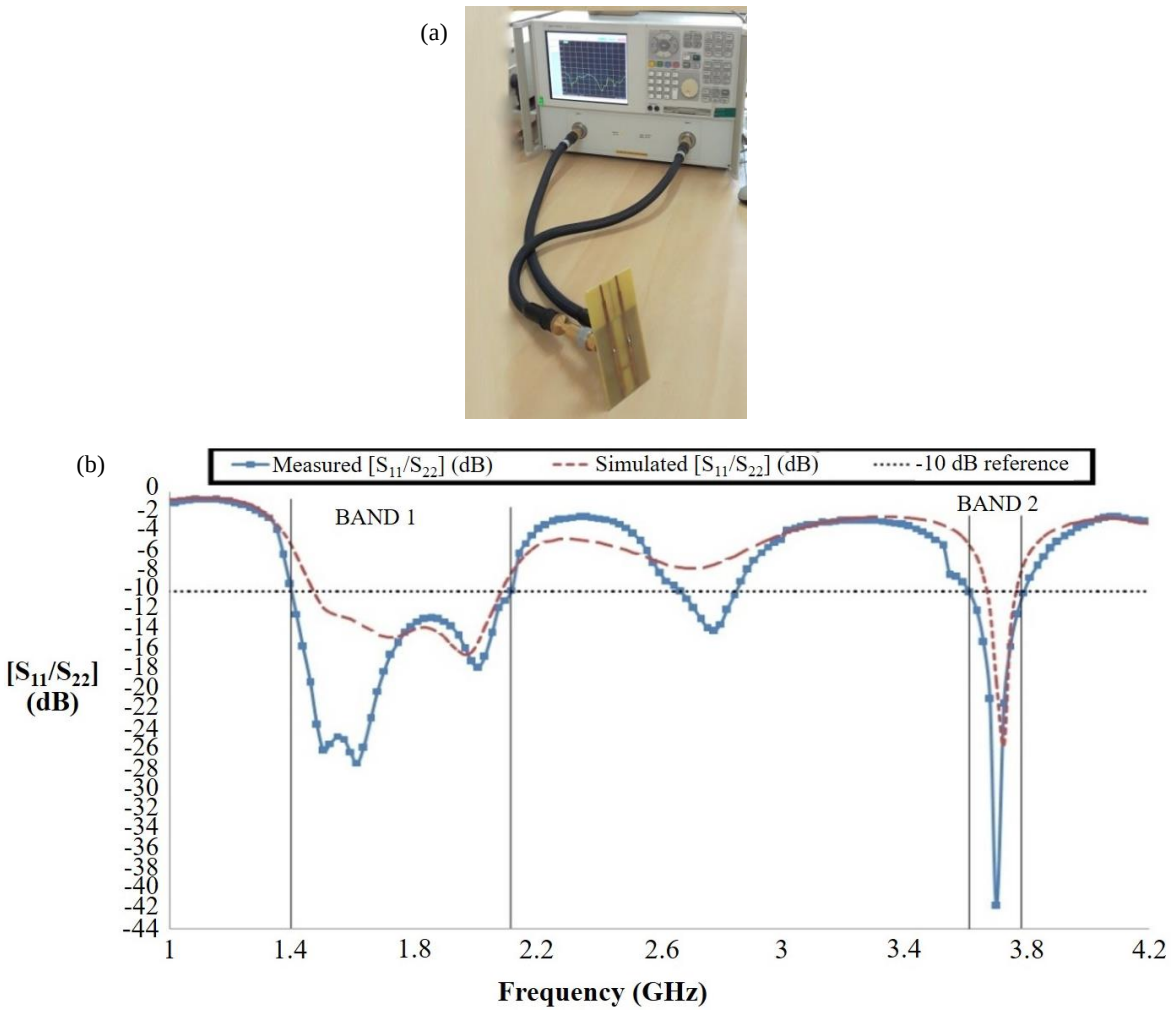

Figure 7 Reflection Coefficient.(a) Experimental setup for measurement, (b) Simulated and measured S_{11}/S_{22} characteristics

at 3.7 GHz, covering the spectrum allotted for L1 GPS, GSM-1800, GSM-1900, 3G UMTS, LTE TDD/FDD and 5G NR applications. The measured S_{11}/S_{22}value validated well with the simulated output with slight variations occuring due to minor fabrication errors.

Mutual coupling between identical antenna elements was measured next using the same experimental setup as illustrated in Figure 7a. Figure 8 illustrates a comparitive plot of simulated and measured mutual coupling.It indicates that the measured result validates the simulated results well. Isolation of better than 14.6 dB with maximum isolation of 24.19 dB and isolation better than 15.7 dB with maximum isolation of 29.2 dB was obtained in first and second range of frequencies, respectively, covering multiple generations of wireless mobile communication.

3.2 Radiation performance

The radiation characteristics of the designed antenna over the azimuth and elevation plane were obtained from the IE3D simulator's output. For measuring the radiation characteristics of the MIMO antenna, the fabricated prototypes were placed inside the non-reflective, echo-free anechoic chamber shown in Figure 9a. Radiation characteristics were recorded in the far field for four frequencies, 1.575 GHz, 1.96 GHz, 2.1 GHz and 3.7 GHz (one sample frequency was taken into consideration from each range of frequencies allotted for various mobile communication generation standards). Figure 9b illustrates the simulated and measured radiation pattern in the azimuth and elevation planes. The antenna exhibits a dumbbell-shaped radiation pattern with almost symmetrical schematics in the elevation plane and almost equal radiation in all direction in the azimuth plane, leading to an omni-directional radiation pattern which is similar to the output obtained from simulated result that is suitable for wireless applications.

Figure 10 illustrates the antenna gain obtained from the simulated and measurement setup. In order to measure the gain, the antennas were placed inside the anechoic chamber. The gain pattern indicates that the designed prototype shows a positive gain value for all the frequencies under consideration with a peak gain of 3.14 dBi obtained at 1.85 GHz. For the range of frequencies under consideration, the obtained gain value is comparable to the peak gain reported for a dual-element MIMO antenna in range of 1.8 to 4.5 dBi [5, 29, 32-33].

Another two-part experiment was conducted to study the effect of coherence between the antennas. In the first scenario, only one port of the transmitting antenna was fed with an input signal that was provided using a Rohde & Schwarz signal generator. The other port was terminated using a 50 ohm matched load. At the receiver end, similar to transmitter side, one antenna port was connected to a Rohde & Schwarz FSP Spectrum analyzer [9 KHz to 30 GHz],

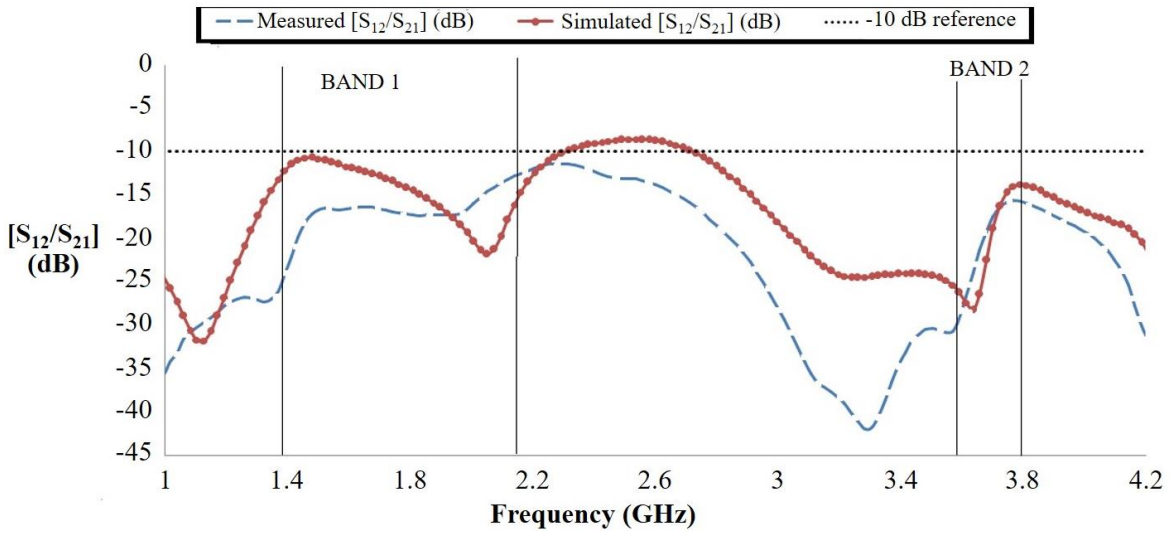

Figure 8 Simulated and measured mutual coupling characteristics

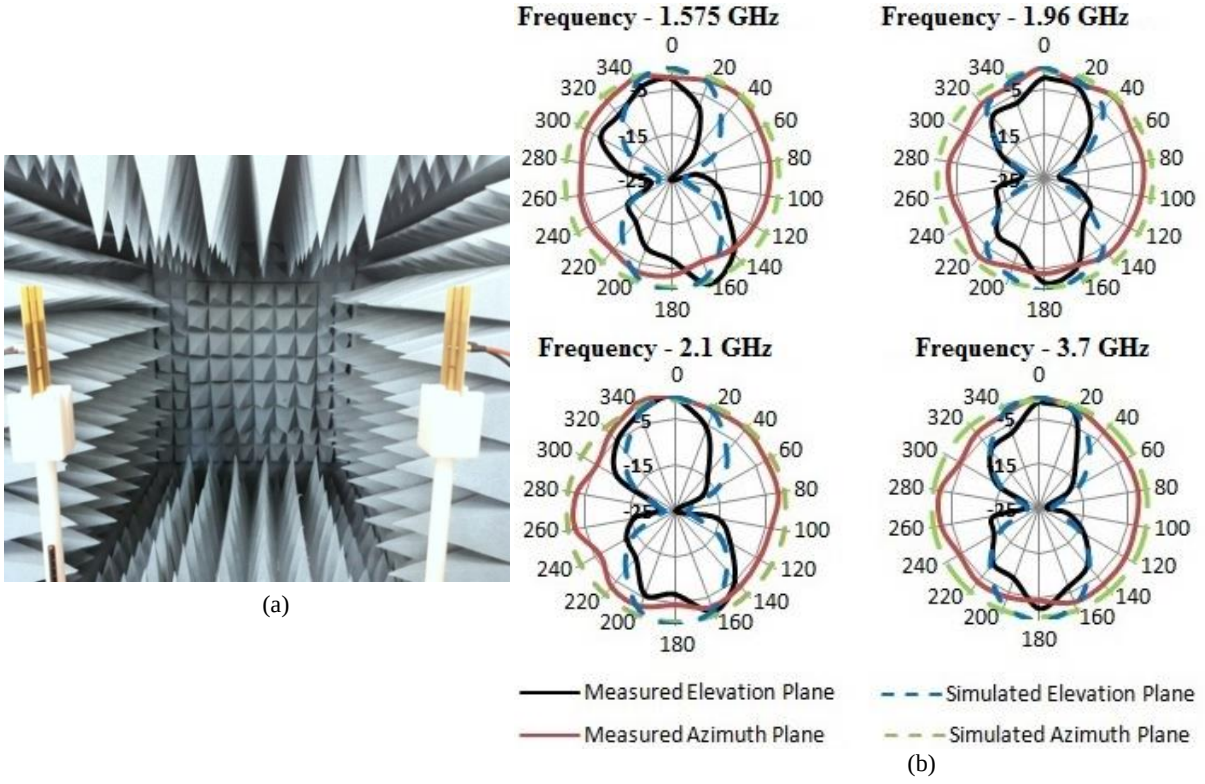

(a)

(b)

Figure 9 (a) MIMO antenna setup inside an anechoic chamber, and (b) Normalized simulated and measured radiation characteristics in elevation and azimuth planes at 1.575 GHz, 1.96 GHz, 2.1 GHz and 3.7 GHz

while the other port was terminated by a matched load of 50 ohms. In the second scenario at the transmitting end, both ports of the MIMO antenna were fed using two signal generators and the receiver end both ports of the antenna were connected to a spectrum analyzer to record the received signal strengths. Figure 11 is a linear plot of the measured signal strength from a spectrum analyzer in both scenarios at 1.96 GHz. It can be observed that the received signal strength measured by the spectrum analyzer when both ports of transmitting antenna were fed with input is higher compared to single input scenario, clearly indicating the presence of constructive coherence.

3.3 Diversity performance

One of the most important benchmarks to evaluate the performance of MIMO antennas is the ECC (ρ) value. This is because it reflects the antenna's diversity performance. ECC measures the correlation between the radiation patterns of identical antenna elements in a MIMO structure. In order to have an optimum performance low correlation is desired. Any value of ECC less than 0.5 is considered adequate in the 3GPP industrial standard specifications [10, 34].

The value of correlation coefficients for an antenna with two elements can be calculated using the scattering

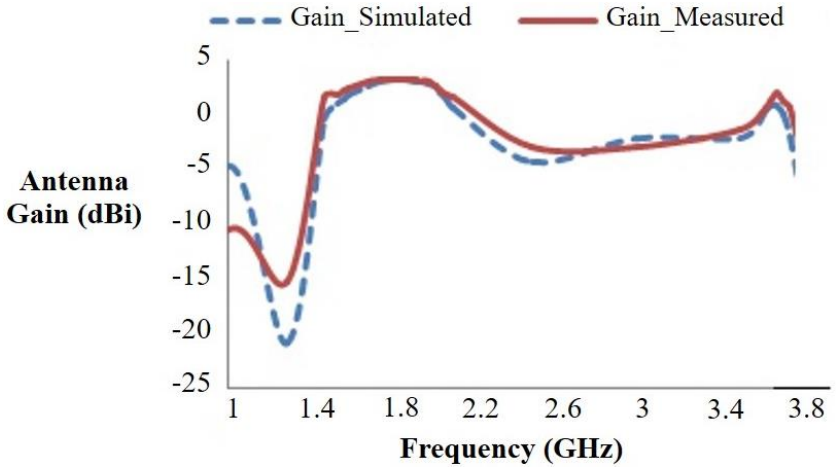

Figure 10 Simulated and measured antenna gains for the designed dual-element MIMO antenna

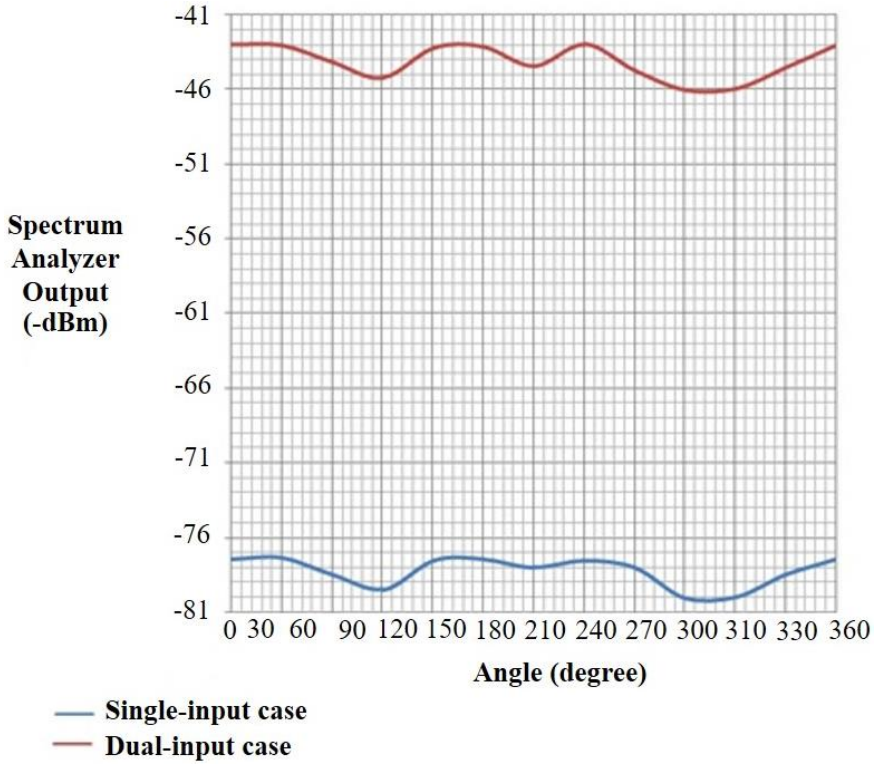

Figure 11 Comparative plots of received signal strength measured through spectrum analyzer

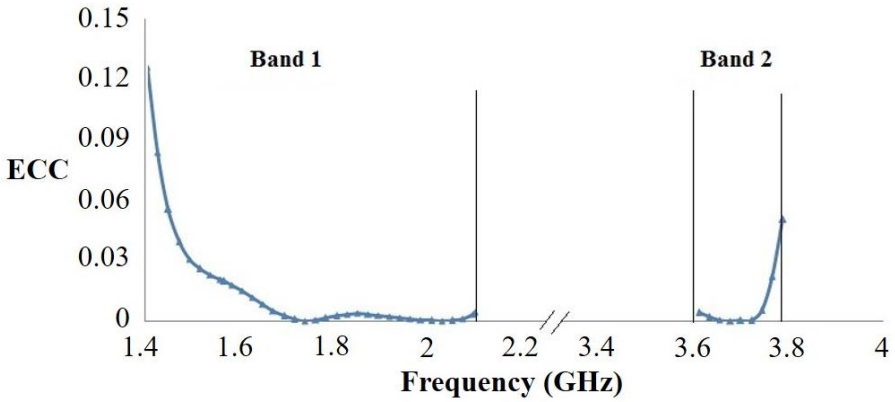

Figure 12 ECC value of the proposed antenna over the two frequency ranges

Table 2 Comparison of proposed antenna with published data

Reference	Year	Antenna Configuration	Supported Generation	S-para reference	Substrate details	ECC value less than
Proposed	2019	MIMO	GPS, 2G, 3G, LTE and 5G	-10 dB	FR4 substrate, ε_r -4.4, h -1.6mm, tan δ-0.02	0.12 in first band, 0.06 in second band
[3]	2017	MIMO	2G,3G, LTE	-10 dB	FR4 substrate, ε_r - 4.4, h -1.6mm, tan δ-0.02	0.05
[5]	2018	MIMO	LTE, 5G	-10 dB	FR4 substrate, ε_r - 4.6, h -0.25 mm, tan δ-0.0025	0.05
[6]	2018	MIMO	LTE, 5G	-6 dB	FR4 substrate, ε_r - 4.4, h -0.8 mm, tan δ-0.02	0.02
[14]	2019	MIMO	LTE, 5G	-6 dB	FR4 substrate, ε_r - 4.4, h -0.8 mm, tan δ-0.02	0.15
[23]	2018	SISO	GPS, 2G, 3G, LTE and 5G	-6 dB	FR4 substrate, ε_r - 4.3, h -0.5 mm, tan δ-0.02	Not applicable
[24]	2018	SISO	LTE	-6 dB	PCB ε_r - 4.4, h -0.8 mm, tan δ-0.02	Not applicable
[29]	2017	MIMO	GPS, 2G, 3G, LTE	-6 dB	FR4 substrate, ε_r - 4.4, h -0.8 mm, tan δ-0.02	0.318
[30]	2018	MIMO	LTE,5G	-10 dB	Nickel silver of conductivity 4 x10^6 S/m, h- 0.3mm	Not mentioned

parameters method employing equation (2) below:

$$\rho = \frac{|S_{11}{}^{*}S_{12} + S_{21}{}^{*}S_{22}|^2}{(1-|S_{11}|^2-|S_{21}|^2)(1-|S_{22}|^2-|S_{12}|^2)} \quad (2)$$

Figure 12 illustrates the computed ECC value at the respective frequencies for designed antenna. It can be observed that the peak value of ECC for the designed antenna is less than 0.12 for all frequencies under consideration in the first band. In the second band, the value of ECC is less than 0.06. Both are much below the acceptable industrial standard value of 0.5.

3.4 Comparison with published work

Table 2 compares the proposed multiband multi-generation compatible MIMO antenna with previously published values. This clearly indicates that the proposed work, owing to its MIMO functionality, good diversity performance and capability to work in multiple mobile communication generations, stands out from other research in this field.

4. Conclusions

The dual-element planar monopole MIMO antenna system presented in this paper can be used to cover multiple mobile communication standards including L1 GPS (1.575 GHz), 2G standards like GSM-1800 (DCS) and GSM-1900 (PCS), 3G standard like UMTS (2.1 GHz), several 4G LTE bands (working on both TDD and FDD technology) and multiple 5G New Radio frequencies. Non-uniform width monopole strips are used as the radiating elements. A hybrid technique comprising of three steps is employed to reduce the mutual coupling below the threshold value of -10 dB and enhance impedance bandwidth to cover the frequencies under consideration. In the desired bands, the Envelop Correlation Coefficient is much lower than the industrial standard of 0.5. The omni-directional radiation pattern and positive gain in the operational bands enables the antenna to be successfully integrated within multi-generation compatible wireless devices.

5. References

[1] Vora LJ. Evolution of mobile generation technology: 1G to 5G and review of upcoming wireless technology 5G. Int J Mod Trends Eng Res. 2015; 2(10):281-90.

[2] Biswas A, Chowdhury M. Wireless communication: theory and applications. Cambridge: Cambridge University Press; 2017.

[3] Agarwal T, Srivastava S. Compact MIMO antenna for multiband mobile applications. J Microw Optoelectron Electromagn Appl. 2017;16(2):542-52.

[4] Dioum I, Diallo A, Farassi AM, Luxey C. A novel compact dual-band LTE antenna system for MIMO operation. IEEE Trans Antenn Propag. 2014; 62(4):2291-6.

[5] Alsaif H, Usman M, Chugtai MT, Nasir J. Cross polarized 2x2 UWB-MIMO antenna system for 5G wireless applications. Prog Electromagn Res M. 2018; 76:157-66.

[6] Zhang W, Weng Z, Wang L. Design of a dual-band MIMO antenna for 5G smartphone application. IEEE International Workshop on Antenna Technology; 2018 Mar 5-7; Nanjing, China. USA: IEEE; 2018. p. 1-3.

[7] 3rd Generation Partnership Project. 5G, NR, User Equipment (UE) radio transmission and reception, Part1 Range 1 Standalone. TS 38.101-1 version 15.2.0 Release 15, July 2018.
[8] 3rd Generation Partnership Project. 5G, NR, Base Station (BS) radio transmission and reception. TS 38.104 version 15.3.0 Release 15, October 2018.
[9] Ban YL, Li C, Sim CYD, Wu G, Wong KL. 4G/5G multiple antennas for future multi-mode smartphone applications. IEEE Access. 2016;4:2981-8.
[10] Votis C, Tatsis G, Kostarakis P. Envelope correlation parameter measurements in a MIMO antenna array configuration. Int J Comm Netw Syst Sci. 2010; 3(4):350-4.
[11] Janaswamy R. Effect of element mutual coupling on the capacity of fixed length linear arrays. IEEE Antenn Wireless Propag Lett. 2002;1:157-60.
[12] Zhang S, Lau BK, Tan Y, Ying Z, He S. Mutual coupling reduction of two PIFAs with a T-Shape slot impedance transformer for MIMO mobile terminals. IEEE Trans Antenn Propag. 2012;60(3):1521-31.
[13] Li Y, Sim CYD, Luo Y, Yang G. High-isolation 3.5-GHz eight-antenna MIMO array using balanced open slot antenna element for 5G Smartphones. IEEE Trans Antenn Propag. 2019;67(6):3820-30.
[14] Jiang W, Liu B, Cui Y, Hu W. High-isolation eight-element MIMO array for 5G Smartphone applications. IEEE Access. 2019;7:34104-12.
[15] Marzudi WNNW, Abidin ZZ, Muji SZ, Yue M, Alhameed RAA. Minimization of mutual coupling using neutralization line technique for 2.4 GHz wireless applications. Int J Digit Inform Wireless Comm. 2014;4(3):292-8.
[16] Chen WS, Chang YL. Small size 5G C-band/WLAN 5.2/5.8GHz MIMO antenna for laptop computer applications. IEEE International Workshop on Electromagnetics: Applications and Student Innovation Competition (iWEM); 2018 Aug 29-31; Nagoya, Japan. USA: IEEE; 2018. p. 1-2.
[17] Bilal M, Saleem R, Abbasi HH, Shafique MF, Brown AK. An FSS-based nonplanar quad-element UWB-MIMO antenna system. IEEE Antenn Wireless Propag Lett. 2017;16:987-90.
[18] Ding CF, Zhang XY, Xue CD, Sim CYD. Novel pattern-diversity-based decoupling method and its application to multi element MIMO antenna. IEEE Trans Antenn Propag. 2018;66(10):4976-85.
[19] Liu H, Li R, Pan Y, Quan X, Yang L, Zheng L. A multi-broadband planar antenna for GSM/UMTS/LTE and WLAN/WiMAX handsets. IEEE Trans Antenn Propag. 2014;62(5):2856-60.
[20] Chen H, Zhao A. LTE antenna design for mobile phone with metal frame. IEEE Antenn Wireless Propag Lett. 2016;15:1462-5.
[21] Wang Y, Du Z. Wideband monopole antenna with less non ground portion for octa-band WWAN/LTE mobile phones. IEEE Trans Antenn Propag. 2016;64(1): 383-8.
[22] Biswas A, Gupta VR. A multiband antenna design for Long Term Evolution (LTE) application. International Conference on Signal Processing and Communication Engineering Systems; 2015 Jan 2-3; Guntur, India. USA: IEEE; 2015. p. 210-4.
[23] Khalilabadi AJ, Zadelgol A. Multiband antenna for wireless applications including GSM/UMTS/LTE and 5G bands. International Applied Computational Electromagnetics Society Symposium (ACES); 2018 Mar 25-29; Denver, USA. USA: IEEE; 2018. p. 1-2.
[24] Huang D, Du Z. Eight-band antenna with a small ground clearance for LTE metal-frame mobile phone applications. IEEE Antenn Wireless Propag Lett. 2018;17(1):34-7.
[25] Biswas A, Gupta VR. Novel compact antenna for Smartphone covering fifteen LTE bands. IEEE International Conference on Electrical, Communication, Electronics, Instrumentation and Computing; 2019 Jan 30-31; Kanchipuram, India.
[26] Toktas A, Akdagli A. Wideband MIMO antenna with enhanced isolation for LTE, WiMAX and WLAN mobile handsets. Electron Lett. 2014;50(10): 723-4.
[27] Yang Y, Chu Q, Mao C. Multiband MIMO antenna for GSM, DCS and LTE indoor applications. IEEE Antenn Wireless Propag Lett. 2016;15:1573-6.
[28] Zhang S, Ying Z, Xiong J, He S. Ultrawideband MIMO/Diversity antennas with tree-like structure to enhance wideband isolation. IEEE Antenn Wireless Propag Lett. 2009;8:1279-82.
[29] Dong J, Yu. X, Deng L. A decoupled multiband dual-antenna system for WWAN/LTE smartphone applications. IEEE Antenn Wireless Propag Lett. 2017;16:1528-32.
[30] Fakih M, Diallo A, Thuc PL, Staraj R, Rachid E, Murad O. A dual band PIFA for MIMO half-duplex 4G and future full-duplex 5G communication for mobile handsets. IEEE Conference on Antenna Measurements & Applications (CAMA); 2018 Sep 3-6; Vasteras, Sweden. USA: IEEE; 2018. p. 1-4.
[31] Ding Z, Yao T, Liu X, Wang X, Liu Z. An eight port dual-band antenna array for 5G smartphone applications. Cross Strait Quad-Regional Radio Science and Wireless Technology Conference (CSQRWC); 2018 Jul 21-24; Xuzhou, China. USA: IEEE; 2018. p. 1-2.
[32] Kumari T, Das G, Sharma A, Gangwar RK. Design approach for dual element hybrid MIMO antenna arrangement for wideband applications. Int. J. RF Microw. Comput.-aided Eng. 2018;29:1-10.
[33] Wang S, Du ZW. Decoupled dual-antenna system using crossed neutralization lines for LTE/WWAN Smartphone applications. IEEE Antenn Wireless Propag Lett, 2015; 14:523-526.
[34] Sharawi MS. Printed MIMO antenna systems: performance metrics, implementations and challenges. Forum for Electromagnetic Research Methods and Application Technologies. 2014;1:1-11.